UNIVERSITÀ DELLA CALABRIA
DIPARTIMENTO DI FISICA

CiP 2026
1° Conferenza Italiana Plasmi

Revisiting X-ray polarization of the shell of Cassiopeia A using spectropolarimetric analysis

A. Mercuri[1], E. Greco[2,3], J. Vink[3], R. Ferrazzoli[4], and S. Perri[1]

1. Università della Calabria, via P. Bucci, cubo 33C, 87036, Rende (CS), Italy
2. INAF - Osservatorio Astronomico di Palermo, Piazza del Parlamento 1, 90134 Palermo, Italy
3. Anton Pannekoek Institute for Astronomy & GRAPPA, University of Amsterdam, Science Park 904, 1098 XH Amsterdam, The Netherlands
4. INAF - Istituto di Astrofisica e Planetologia Spaziali, Via del Fosso del Cavaliere 100, 00133 Roma, Italy

Introduction:
Supernova Remnants (SNRs) and X-ray Emission

SNRs are the diffuse remains of supernova explosions, marking the violent deaths of massive stars or white dwarfs.

X-ray spectroscopy → **study of the interaction between SNRs and the Interstellar / circumstellar medium (ISM/CSM).**

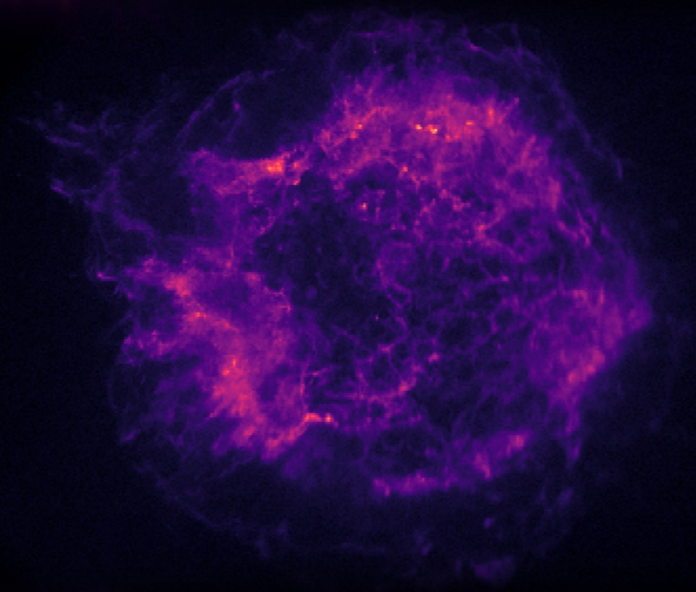

Introduction:
Supernova Remnants (SNRs) and X-ray Emission

SNRs are the diffuse remains of supernova explosions, marking the violent deaths of massive stars or white dwarfs.

X-ray spectroscopy → **study of the interaction between SNRs and the Interstellar / circumstellar medium (ISM/CSM).**

X-ray emission:

- **Thermal X-ray emission**:
  - Arises from heated **electrons** and **ions**.
  - Originates from stellar ejecta (reverse shock) or swept-up ISM/CSM (forward shock).
- **Nonthermal synchrotron X-ray emission**:
  Caused by **relativistic electrons accelerated at the shock front** and making a spiral motion around magnetic field lines.

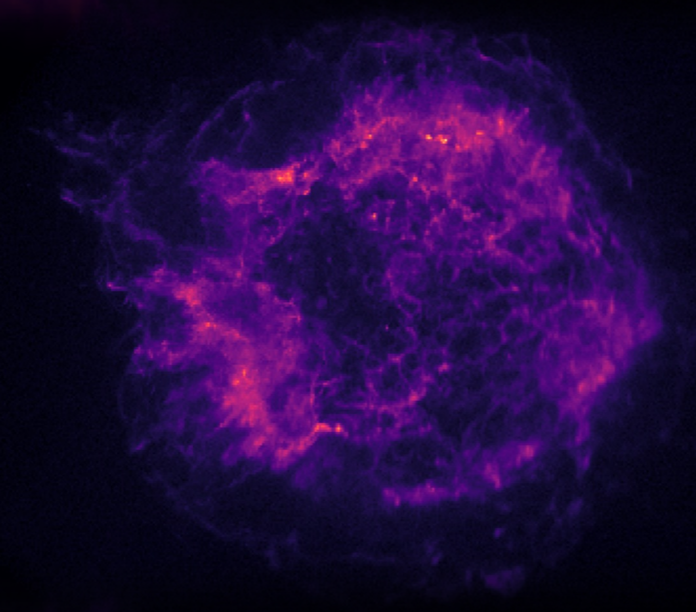

Introduction:

Supernova Remnants (SNRs) and X-ray Emission

SNRs are the diffuse remains of supernova explosions, marking the violent deaths of massive stars or white dwarfs.

X-ray spectroscopy → **study of the interaction between SNRs and the Interstellar / circumstellar medium (ISM/CSM)**.

Polarization in X-ray Emission:

- **Highly polarized nonthermal radiation** (up to **70%–75%**), providing insight into magnetic field structures.
- **Magnetic turbulence** can reduce polarization.

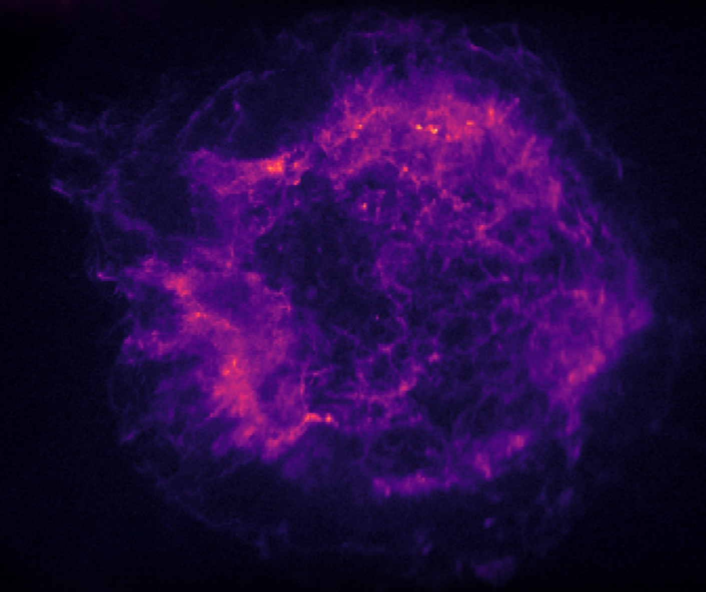

Introduction:

Cassiopeia A (Cas A)

Imaging X-ray Polarimetry Explorer (IXPE) Mission:

- First telescope capable of measuring X-ray polarization (NASA & ASI collaboration).
- Angular resolution: ~30" in the 2–8 keV band.
- Enables spatially resolved spectropolarimetric analysis of **Stokes parameters I, Q, and U.**

Introduction:

Cassiopeia A (Cas A)

Imaging X-ray Polarimetry Explorer (IXPE) Mission:

- First telescope capable of measuring X-ray polarization (NASA & ASI collaboration).
- Angular resolution: ~30" in the 2–8 keV band.
- Enables spatially resolved spectropolarimetric analysis of **Stokes parameters I, Q, and U.**

Polarization Findings (Vink et al. 2022):

- Detected polarized X-ray emission (3–6 keV range).
- Overall **polarizarion degree (PD)**: ~2.5%, up to 5% in the forward shock.
- Magnetic Field: Radially oriented.

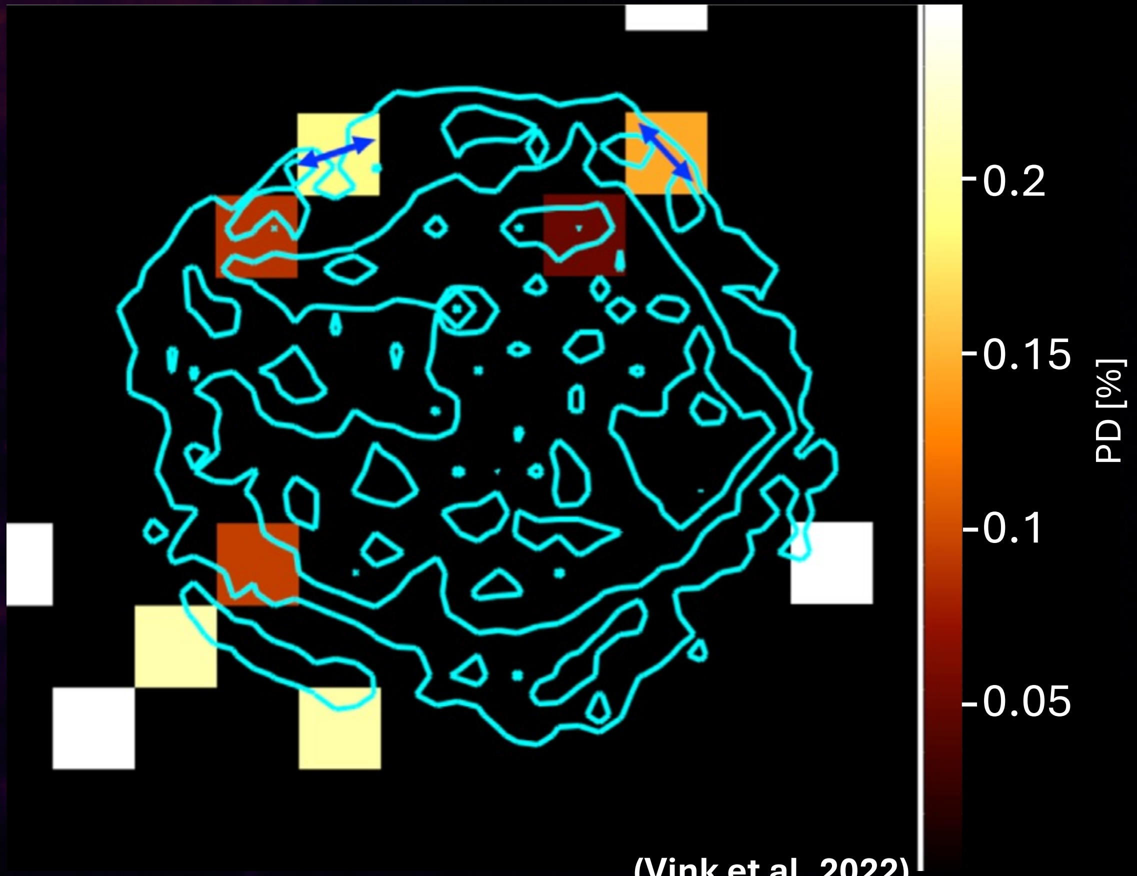

(Vink et al. 2022)

Introduction:

Spectropolarimetric Analysis of Cas A

Objective: Analyze X-ray polarization properties in the Cassiopeia A supernova remnant, focusing on shell regions dominated by nonthermal synchrotron emission.

Introduction:

Spectropolarimetric Analysis of Cas A

Objective: Analyze X-ray polarization properties in the Cassiopeia A supernova remnant, focusing on shell regions dominated by nonthermal synchrotron emission.

IXPE offers unique insights into X-ray polarization.

IXPE Limitations: IXPE's spectral resolution (30 arcsec) is insufficient to resolve detailed features, such as the continuum and emission lines.

Introduction:

Spectropolarimetric Analysis of Cas A

Objective: Analyze X-ray polarization properties in the Cassiopeia A supernova remnant, focusing on shell regions dominated by nonthermal synchrotron emission.

IXPE offers unique insights into X-ray polarization.

IXPE Limitations: IXPE's spectral resolution (30 arcsec) is insufficient to resolve detailed features, such as the continuum and emission lines.

Solution: Combine high spatial and spectral resolution (0.5 arcsec) data from *Chandra* to constrain thermal emission.

Introduction:

Region Selection for Polarization Analysis

Objective: Analyze X-ray polarization properties in the Cassiopeia A supernova remnant, focusing on shell regions dominated by nonthermal synchrotron emission.

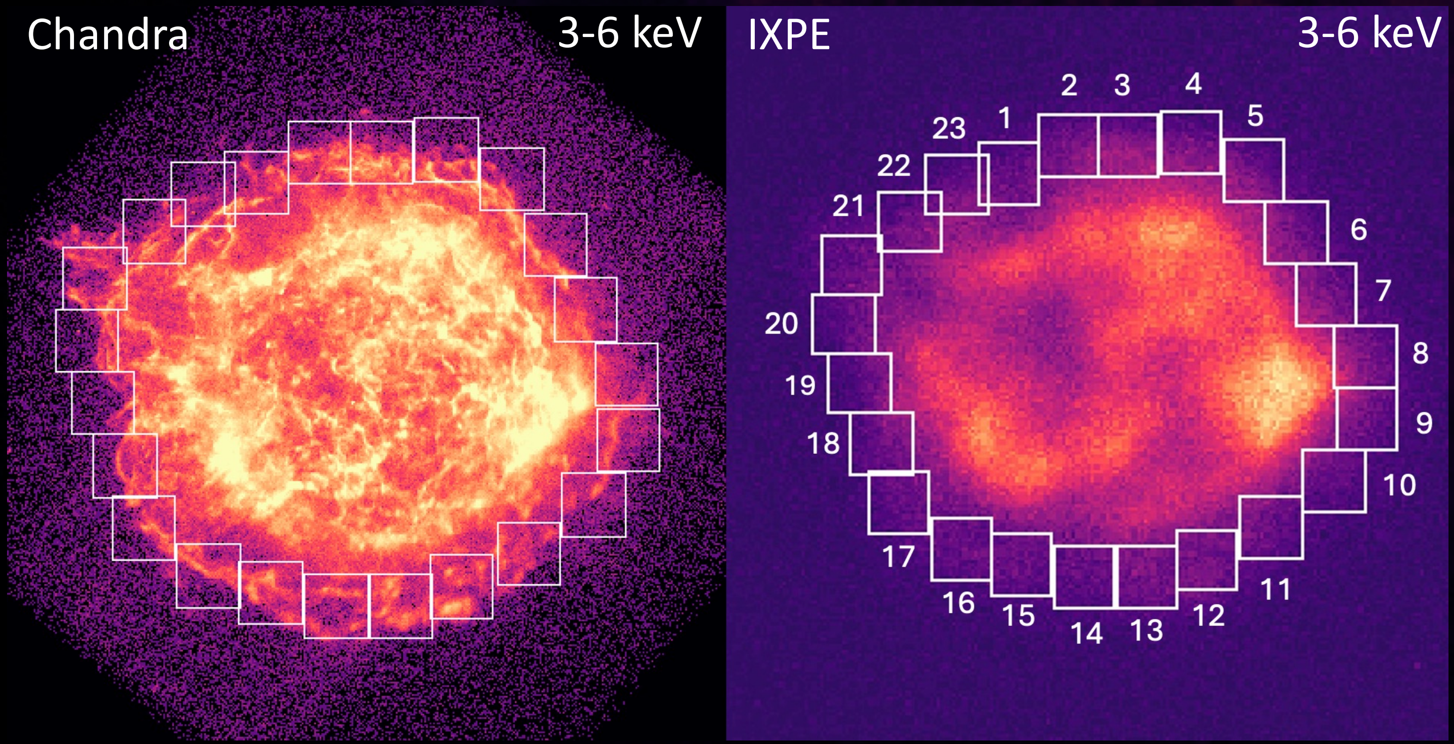

23 regions (42”x42”) selected across Cas A’s shell.

1. **Minimized contamination** between adjacent regions (**IXPE resolution**).
2. **Sufficient photon statistics** for reliable polarization analysis.
3. **Reduced thermal contamination** from ejecta & mixed polarization angles.

How to estimate the thermal contribution?

We use Chandra as a "calibration" for the thermal contribution to be incorporated into IXPE, fitting each region individually.

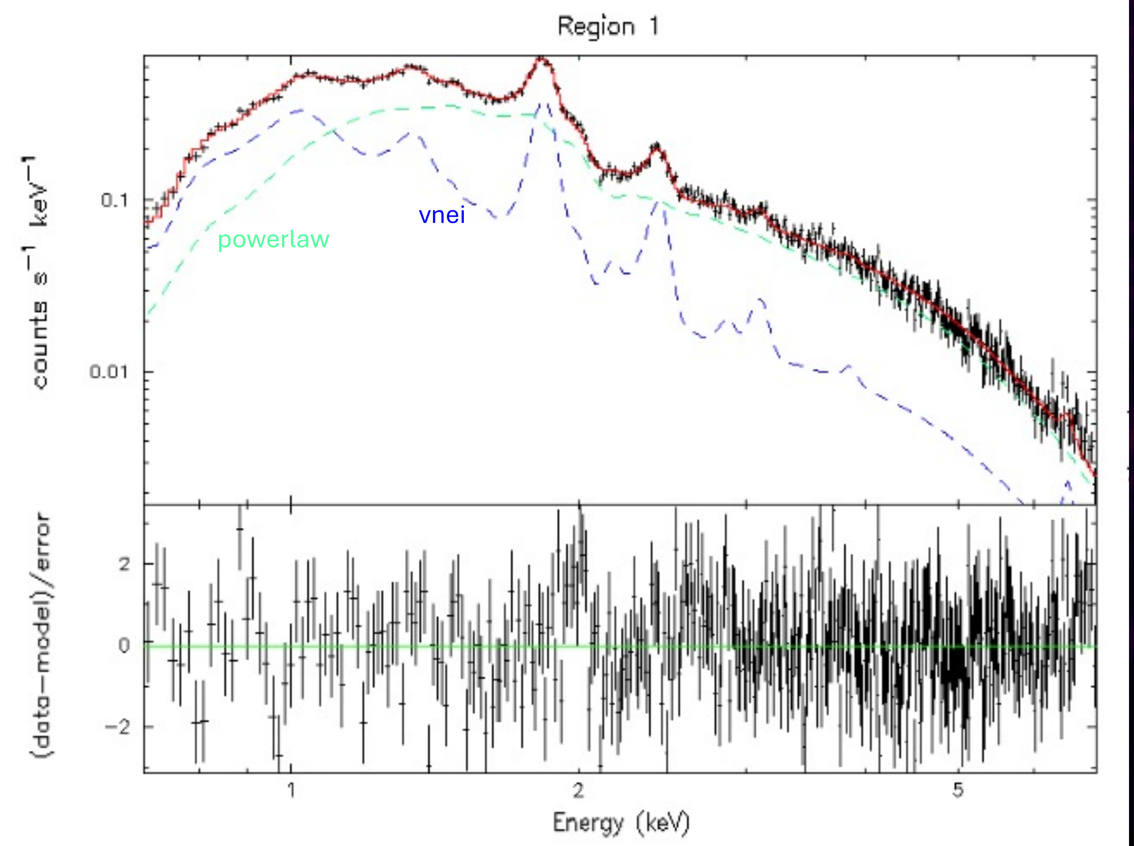

Emission lines are present in the spectra, indicating thermal contamination from either ejecta or ISM/CSM.

Chandra Spectral Fitting

Model Used:
TBabs*(vnei+powerlaw)

Absorption

Thermal component

Nonthermal component

IXPE Data Analysis

Constant polarization

IXPE Spectral Fitting

Model Used:
TBabs*(polconst*vnei+polconst*powerlaw).

- **Assumptions:**
  - Thermal component (**vnei**) is **unpolarized** (**PD = 0 for** the **thermal** component).
- **Fixed Parameters:**
  - **nH, kT, Tau, abundances, and vnei normalization** frozen from **Chandra best-fit results**.
- **Energy Band:**
  - **3–6 keV focus**.

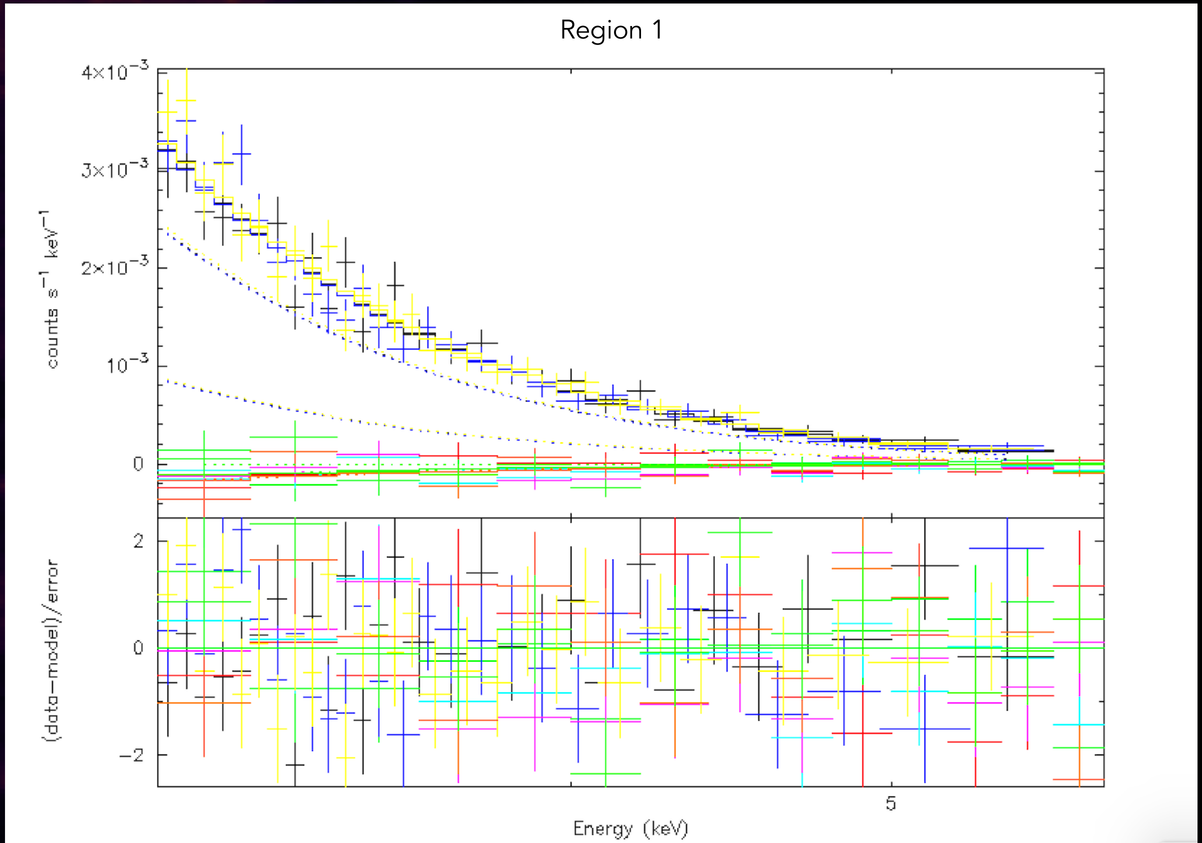

IXPE Data Analysis

Constant polarization

IXPE Spectral Fitting

Model Used:
TBabs*(polconst*vnei+polconst*powerlaw).

•Assumptions:

- Thermal component (**vnei**) is **unpolarized** (**PD = 0 for** the **thermal** component).

•Fixed Parameters:

- **nH, kT, Tau, abundances, and vnei normalization** frozen from **Chandra best-fit results**.

•Energy Band:

- **3–6 keV focus**.

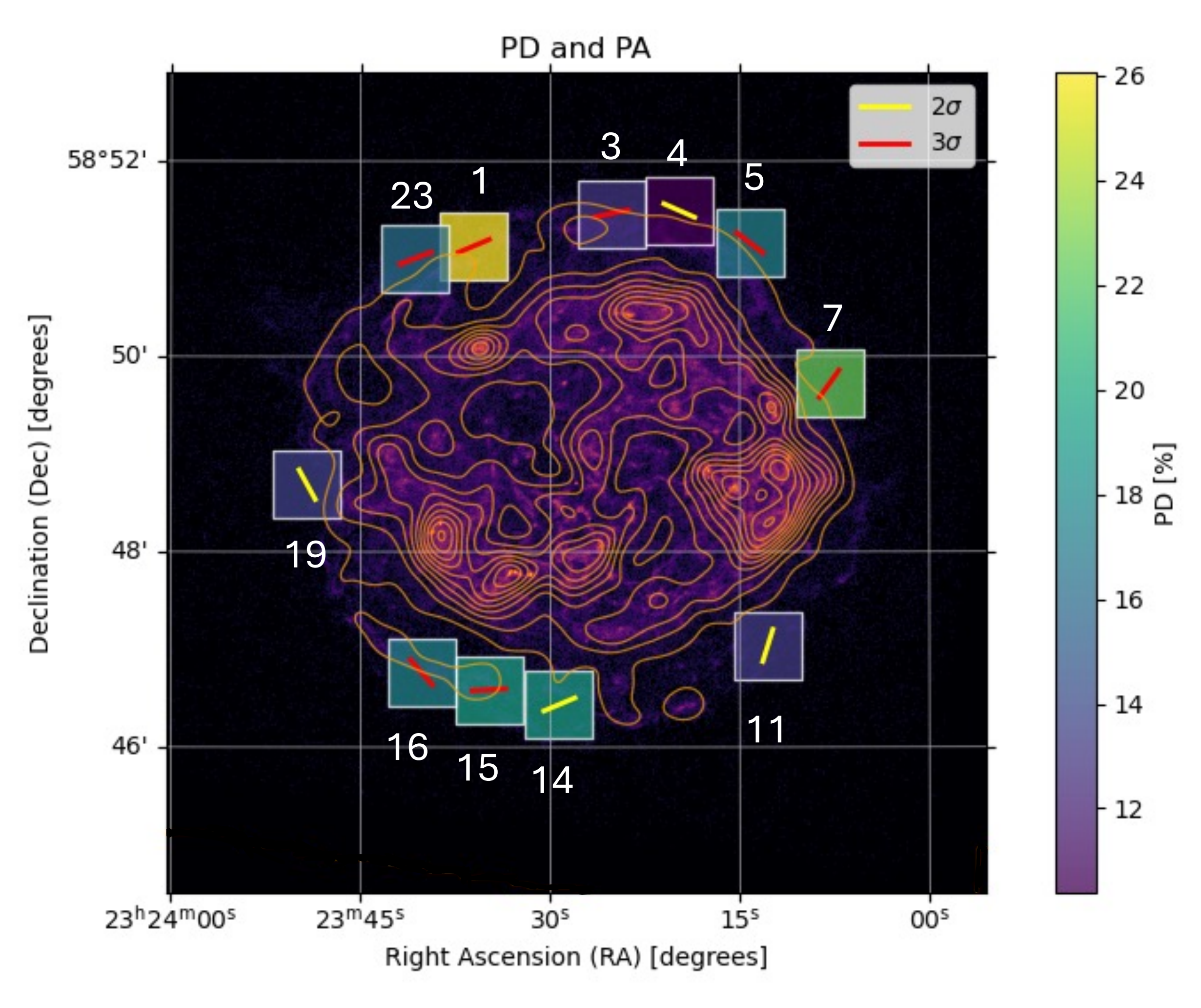

PD ranges from 10% to 26%

IXPE Data Analysis:
Comparison with IXPEOBSSIM

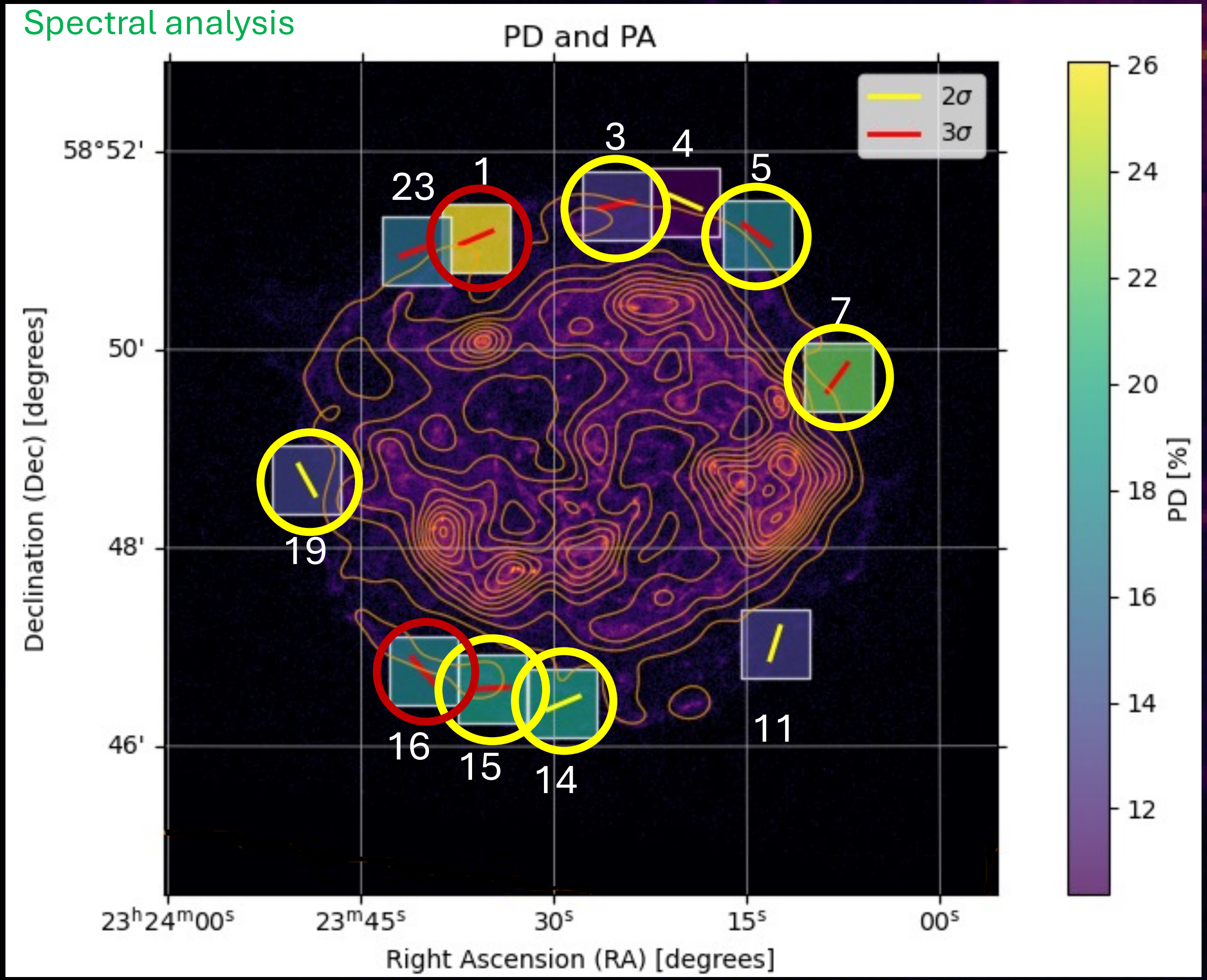

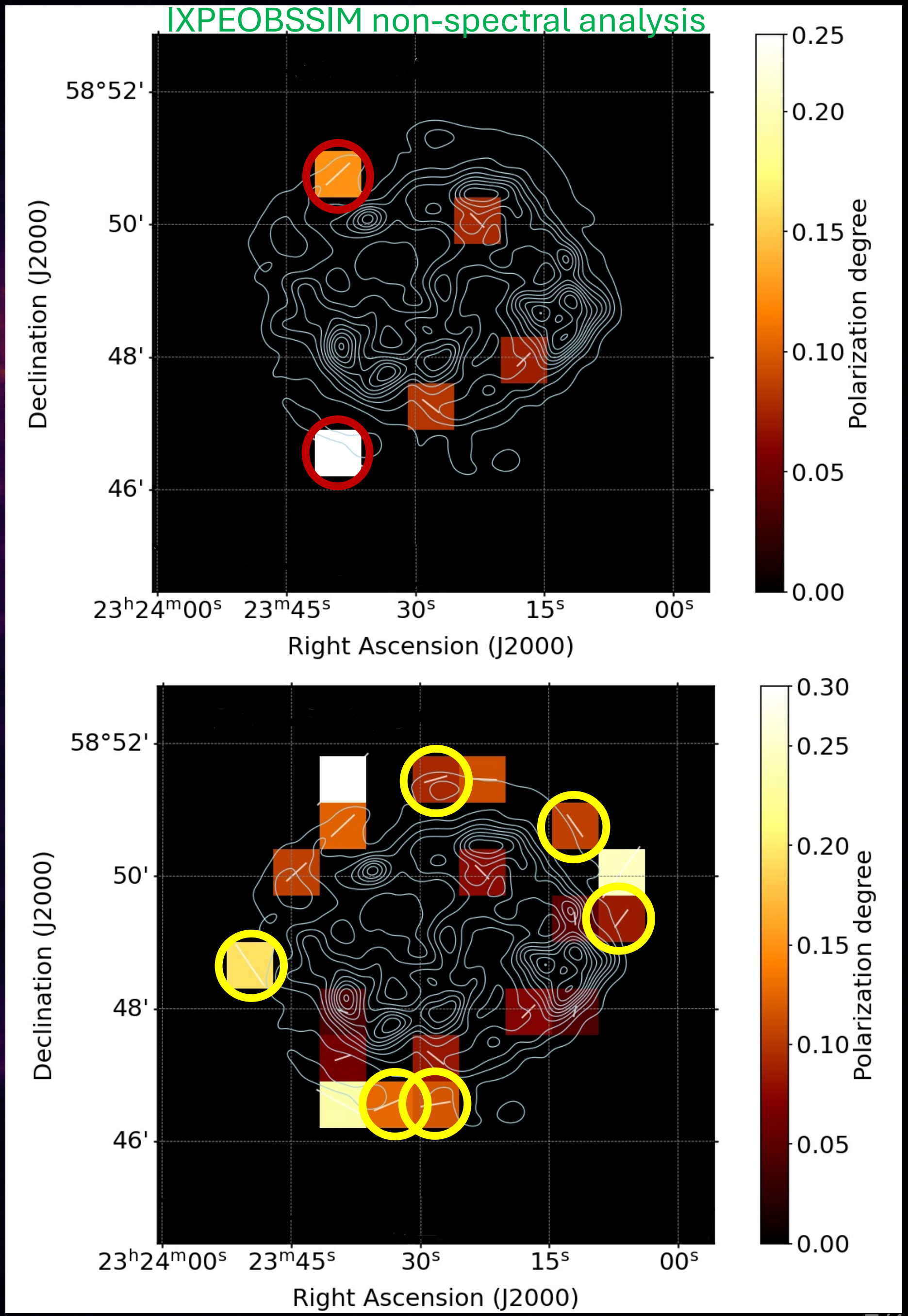

IXPE Data Analysis:
Comparison with IXPEOBSSIM

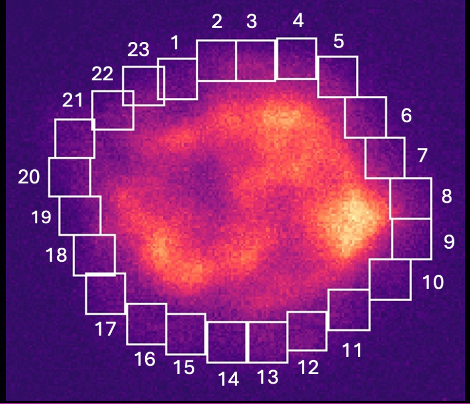

Region	***Spectropolarimetric analysis***			***IXPEOBSSIM analysis***			
	PD (%)	***PA (°)***	***σ***	***PD (%)***	***PD_corr (%)***	***PA (°)***	***σ***
1	26.06 ±6.80	-67.21 ±7.47	3,83	20.56 ±3.82	22.98 ±4.27	-71.54 ±7.12	4,02
3	12.91 ±4.19	-78.64 ±9.45	3,08	10.64 ±3.82	12.39 ±4.45	-75.95 ±10.27	2,79
4	<22.31	-	2,25	<22.45	<25.40	-	2,36
5	17.32 ±4.95	52.54 ±8.25	3,5	17.16 ±4.52	19.20 ±5.06	47.65 ±7.54	3,8
7	22.47 ±6.81	-35.68 ±8.64	3,3	10.14 ±3.95	11.56 ±4.50	-36.19 ±11.16	2,57
11	<28.35	-	2,24	<25.23	<29.19	-	2,1
14	19.21 ±7.25	-67.14 ±11.09	2,66	<28.05	<30.82	-	2,28
15	19.21 ±5.94	-86.60 ±8.93	3,24	18.57 ±5.62	20.38 ±6.17	-81.19 ±8.68	3,3
16	17.50 ±5.45	41.00 ±9.14	3,21	15.59 ±5.74	17.03 ±6.28	40.72 ±10.57	2,71
19	<28.93	-	2,24	<26.07	<30.79	-	2,42
23	16.09 ±5.30	-69.03 ±9.65	3,04	<24.49	<26.87	-	2,27

IXPE Data Analysis:
Comparison with IXPEOBSSIM

- High significance
- Differences between the analyses
- PA value unaffected by the thermal component

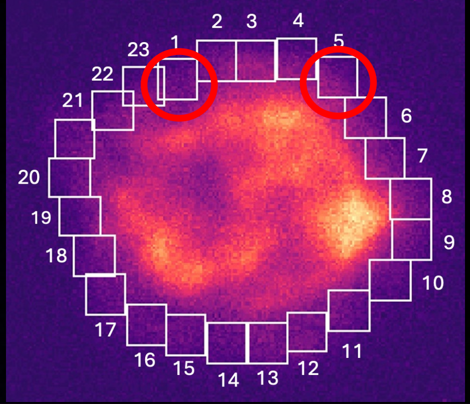

Region	Spectropolarimetric analysis			IXPEOBSSIM analysis			
	PD (%)	**PA (°)**	**σ**	**PD (%)**	**PD_corr (%)**	**PA (°)**	**σ**
1	26.06 ±6.80	-67.21 ±7.47	3,83	20.56 ±3.82	22.98 ±4.27	-71.54 ±7.12	4,02
3	12.91 ±4.19	-78.64 ±9.45	3,08	10.64 ±3.82	12.39 ±4.45	-75.95 ±10.27	2,79
4	<22.31	-	2,25	<22.45	<25.40	-	2,36
5	17.32 ±4.95	52.54 ±8.25	3,5	17.16 ±4.52	19.20 ±5.06	47.65 ±7.54	3,8
7	22.47 ±6.81	-35.68 ±8.64	3,3	10.14 ±3.95	11.56 ±4.50	-36.19 ±11.16	2,57
11	<28.35	-	2,24	<25.23	<29.19	-	2,1
14	19.21 ±7.25	-67.14 ±11.09	2,66	<28.05	<30.82	-	2,28
15	19.21 ±5.94	-86.60 ±8.93	3,24	18.57 ±5.62	20.38 ±6.17	-81.19 ±8.68	3,3
16	17.50 ±5.45	41.00 ±9.14	3,21	15.59 ±5.74	17.03 ±6.28	40.72 ±10.57	2,71
19	<28.93	-	2,24	<26.07	<30.79	-	2,42
23	16.09 ±5.30	-69.03 ±9.65	3,04	<24.49	<26.87	-	2,27

IXPE Data Analysis:
Comparison with IXPEOBSSIM

- High significance
- Differences between the analyses
- PA value unaffected by the thermal component

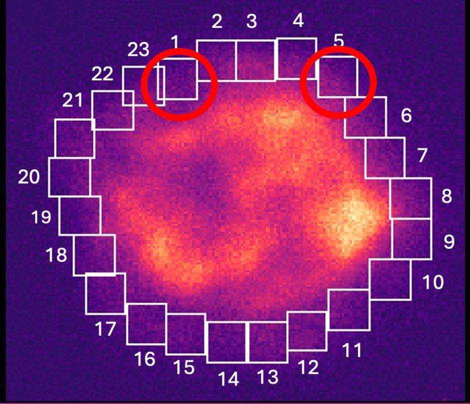

1° Conferenza Italiana Plasmi

Region	Spectropolarimetric analysis			IXPEOBSSIM analysis			
	PD (%)	PA (°)	σ	PD (%)	PD_corr (%)	PA (°)	σ
1	26.06 ±6.80	-67.21 ±7.47	3,83	6 ±3.82	22.98 ±4.27	-71.54 ±7.12	4,02
3	12.91 ±4.19	-78.64 ±9.45	3,08	10.64 ±3.82	12.39 ±4.45	-75.95 ±10.27	2,79
4	<22.31	-	2,25	<22.45	<25.40	-	2,36
5	17.32 ±4.95	52.54 ±8.25	3,5	6 ±4.52	19.20 ±5.06	47.65 ±7.54	3,8
7	22.47 ±6.81	-35.68 ±8.64	3,3	10.14 ±3.95	11.56 ±4.50	-36.19 ±11.16	2,57
11	<28.35	-	2,24	<25.23	<29.19	-	2,1
14	19.21 ±7.25	-67.14 ±11.09	2,66	<28.05	<30.82	-	2,28
15	19.21 ±5.94	-86.60 ±8.93	3,24	18.57 ±5.62	20.38 ±6.17	-81.19 ±8.68	3,3
16	17.50 ±5.45	41.00 ±9.14	3,21	15.59 ±5.74	17.03 ±6.28	40.72 ±10.57	2,71
19	<28.93	-	2,24	<26.07	<30.79	-	2,42
23	16.09 ±5.30	-69.03 ±9.65	3,04	<24.49	<26.87	-	2,27

IXPE Data Analysis:

Comparison with IXPEOBSSIM

- High significance
- Differences between the analyses
- PA value unaffected by the thermal component

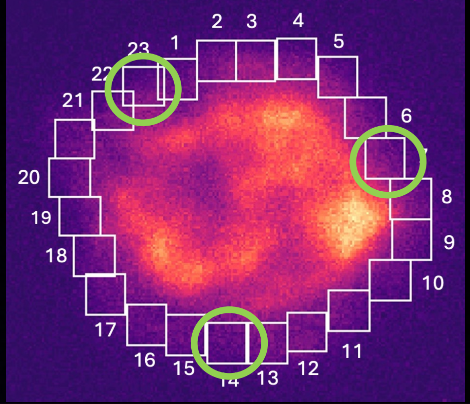

Region	Spectropolarimetric analysis			IXPEOBSSIM analysis			
	PD (%)	PA (°)	σ	PD (%)	PD_corr (%)	PA (°)	σ
1	26.06 ±6.80	-67.21 ±7.47	3,83	20.56 ±3.82	22.98 ±4.27	-71.54 ±7.12	4,02
3	12.91 ±4.19	-78.64 ±9.45	3,08	10.64 ±3.82	12.39 ±4.45	-75.95 ±10.27	2,79
4	<22.31	-	2,25	<22.45	<25.40	-	2,36
5	17.32 ±4.95	52.54 ±8.25	3,5	17.16 ±4.52	19.20 ±5.06	47.65 ±7.54	3,8
7	22.47 ±6.81	-35.68 ±8.64	3,3	10.14 ±3.95	11.56 ±4.50	-36.19 ±11.16	2,57
11	<28.35	-	2,24	<25.23	<29.19	-	2,1
14	19.21 ±7.25	-67.14 ±11.09	2,66	<28.05	<30.82	-	2,28
15	19.21 ±5.94	-86.60 ±8.93	3,24	18.57 ±5.62	20.38 ±6.17	-81.19 ±8.68	3,3
16	17.50 ±5.45	41.00 ±9.14	3,21	15.59 ±5.74	17.03 ±6.28	40.72 ±10.57	2,71
19	<28.93	-	2,24	<26.07	<30.79	-	2,42
23	16.09 ±5.30	-69.03 ±9.65	3,04	<24.49	<26.87	-	2,27

IXPE Data Analysis:
Comparison with IXPEOBSSIM

- High significance
- Differences between the analyses
- PA value unaffected by the thermal component

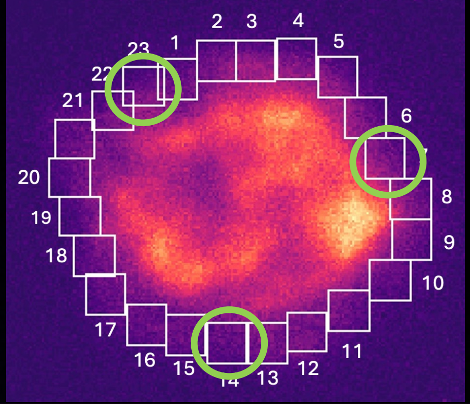

Region	Spectropolarimetric analysis			IXPEOBSSIM analysis			
	PD (%)	PA (°)	σ	PD (%)	PD_corr (%)	PA (°)	σ
1	26.06 ±6.80	-67.21 ±7.47	3,83	20.56 ±3.82	22.98 ±4.27	-71.54 ±7.12	4,02
3	12.91 ±4.19	-78.64 ±9.45	3,08	10.64 ±3.82	12.39 ±4.45	-75.95 ±10.27	2,79
4	<22.31	-	2,25	<22.45	<25.40	-	2,36
5	17.32 ±4.95	52.54 ±8.25	3,5	17.16 ±4.52	19.20 ±5.06	47.65 ±7.54	3,8
7	22.47 ±6.81	-35.68 ±8.64	3,3	10.14 ±3.95	11.56 ±4.50	-36.19 ±11.16	2,57
11	<28.35	-	2,24	<25.23	<29.19	-	2,1
14	19.21 ±7.25	-67.14 ±11.09	2,66	<28.05	<30.82	-	2,28
15	19.21 ±5.94	-86.60 ±8.93	3,24	18.57 ±5.62	20.38 ±6.17	-81.19 ±8.68	3,3
16	17.50 ±5.45	41.00 ±9.14	3,21	15.59 ±5.74	17.03 ±6.28	40.72 ±10.57	2,71
19	<28.93	-	2,24	<26.07	<30.79	-	2,42
23	16.09 ±5.30	-69.03 ±9.65	3,04	<24.49	<26.87	-	2,27

IXPE Data Analysis:

Comparison with IXPEOBSSIM

- High significance
- Differences between the analyses
- PA value unaffected by the thermal component

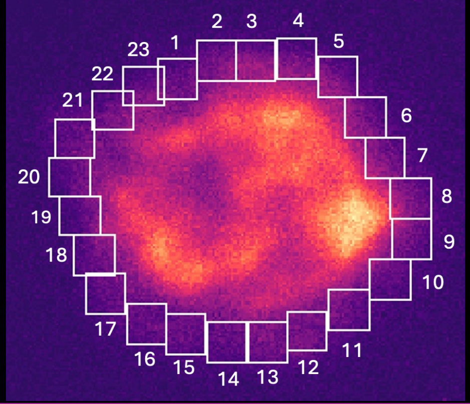

Region	***Spectropolarimetric analysis***			***IXPEOBSSIM analysis***			
	PD (%)	***PA (°)***	***σ***	***PD (%)***	***PD_corr (%)***	***PA (°)***	***σ***
1	26.06 ±6.80	-67.21 ±7.47	3,83	20.56 ±3.82	22.98 ±4.27	-71.54 ±7.12	4,02
3	12.91 ±4.19	-78.64 ±9.45	3,08	10.64 ±3.82	12.39 ±4.45	-75.95 ±10.27	2,79
4	<22.31	-	2,25	<22.45	<25.40	-	2,36
5	17.32 ±4.95	52.54 ±8.25	3,5	17.16 ±4.52	19.20 ±5.06	47.65 ±7.54	3,8
7	22.47 ±6.81	-35.68 ±8.64	3,3	10.14 ±3.95	11.56 ±4.50	-36.19 ±11.16	2,57
11	<28.35	-	2,24	<25.23	<29.19	-	2,1
14	19.21 ±7.25	-67.14 ±11.09	2,66	<28.05	<30.82	-	2,28
15	19.21 ±5.94	-86.60 ±8.93	3,24	18.57 ±5.62	20.38 ±6.17	-81.19 ±8.68	3,3
16	17.50 ±5.45	41.00 ±9.14	3,21	15.59 ±5.74	17.03 ±6.28	40.72 ±10.57	2,71
19	<28.93	-	2,24	<26.07	<30.79	-	2,42
23	16.09 ±5.30	-69.03 ±9.65	3,04	<24.49	<26.87	-	2,27

IXPE Data Analysis:
Comparison with IXPEOBSSIM

- High significance
- Differences between the analyses
- PA value unaffected by the thermal component

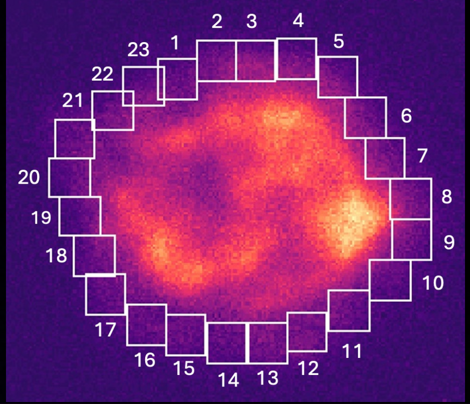

Region	Spectr… …lysis			IXPEOBSSI…			
	PD (%)	PA (°)	σ	PD (%)	PD_corr (%)	PA (°)	σ
1	26.06 ±6.80	-67.21 ±7.47	3,83	20.56 ±3.82	22.98 ±4.27	-71.54 ±7.12	4,02
3	12.91 ±4.19	-78.64 ±9.45	3,08	10.64 ±3.82	12.39 ±4.45	-75.95 ±10.27	2,79
4	<22.31	-	2,25	<22.45	<25.40	-	2,36
5	17.32 ±4.95	52.54 ±8.25	3,5	17.16 ±4.52	19.20 ±5.06	47.65 ±7.54	3,8
7	22.47 ±6.81	-35.68 ±8.64	3,3	10.14 ±3.95	11.56 ±4.50	-36.19 ±11.16	2,57
11	<28.35	-	2,24	<25.23	<29.19	-	2,1
14	19.21 ±7.25	-67.14 ±11.09	2,66	<28.05	<30.82	-	2,28
15	19.21 ±5.94	-86.60 ±8.93	3,24	18.57 ±5.62	20.38 ±6.17	-81.19 ±8.68	3,3
16	17.50 ±5.45	41.00 ±9.14	3,21	15.59 ±5.74	17.03 ±6.28	40.72 ±10.57	2,71
19	<28.93	-	2,24	<26.07	<30.79	-	2,42
23	16.09 ±5.30	-69.03 ±9.65	3,04	<24.49	<26.87	-	2,27

Polarization Degree Distribution

High PD:

- Highest in **southeastern** **and** **northeastern** regions.

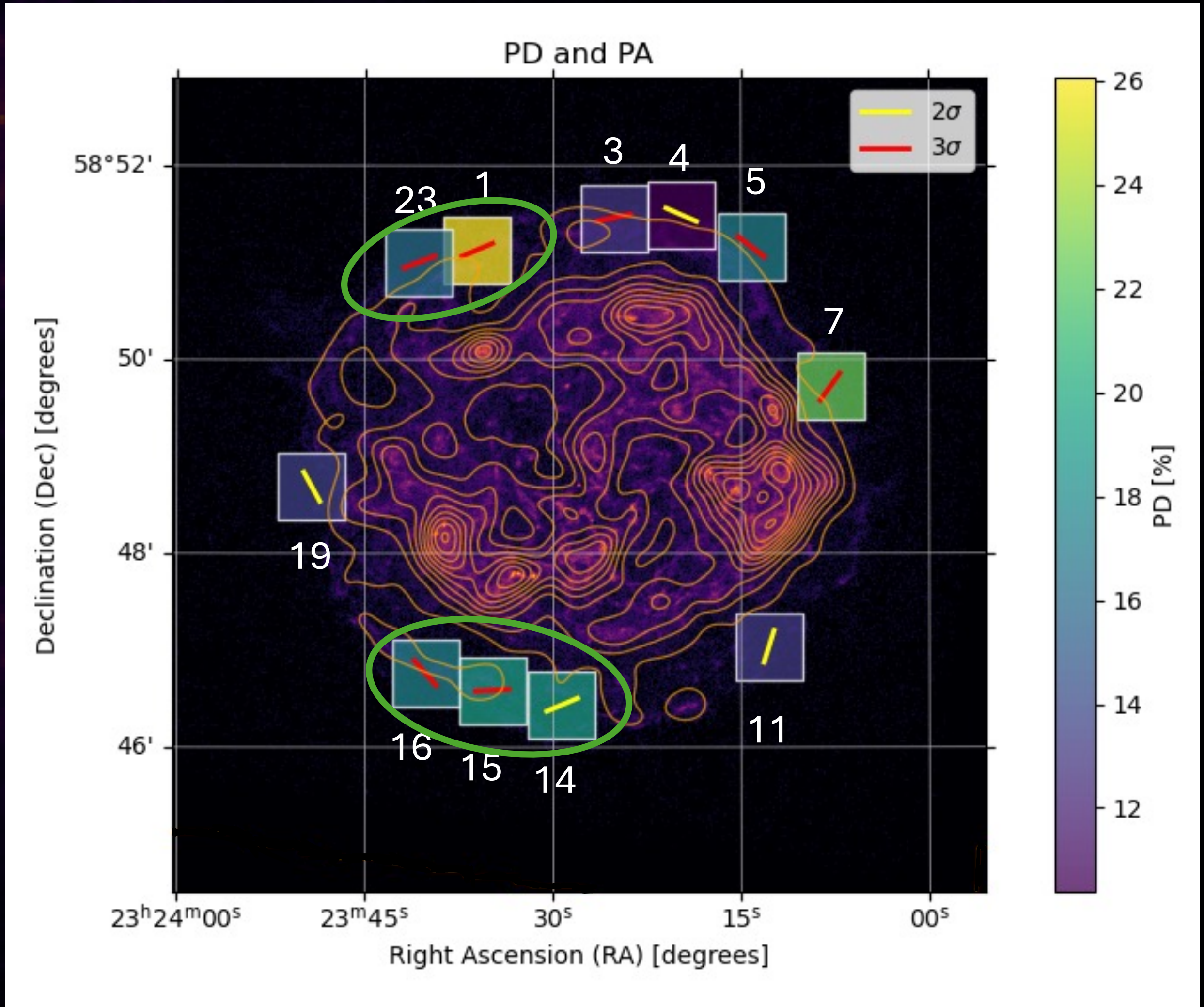

Polarization Degree Distribution

High PD:

•Highest in **southeastern and northeastern** regions.

Low PD Regions:

•Northwestern (Regions 3, 4, 5) → Interaction with **dense CSM shell** (Vink et al. 2022; Orlando et al. 2022) → Causes **secondary reverse shock**, increasing turbulence and reducing PD.

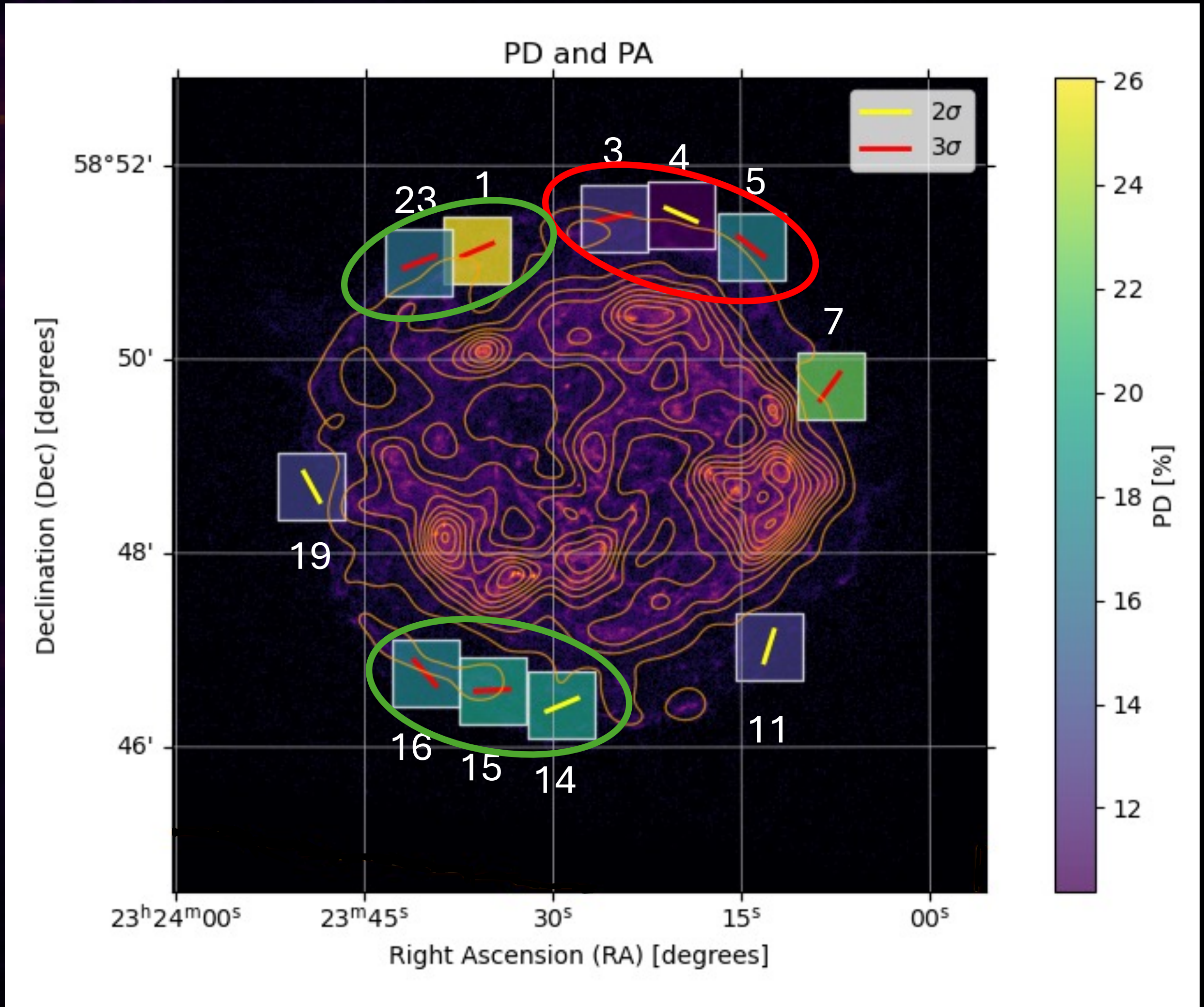

Polarization Degree Distribution

High PD:

•Highest in **southeastern and northeastern** regions.

Low PD Regions:

•Northwestern (Regions 3, 4, 5) → Interaction with **dense CSM shell** (Vink et al. 2022; Orlando et al. 2022) → Causes **secondary reverse shock**, increasing turbulence and reducing PD.

Magnetic Field Alignment:

•Most areas → Radial magnetic field, PA aligned with the shock front.

•Regions 7 & 11 (West) → **Non-radial fields** due to **counter-jet and reverse shock interactions**.

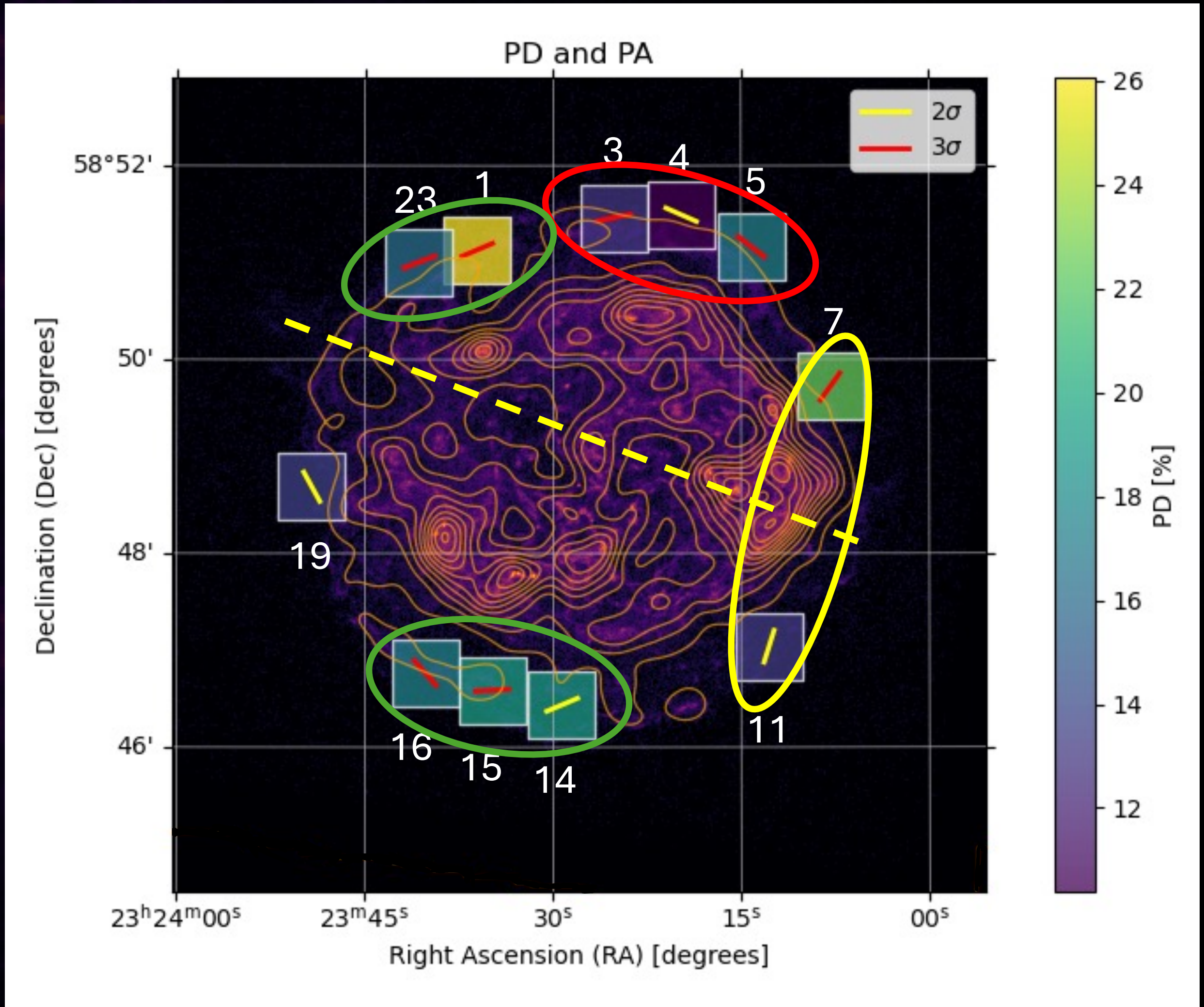

Estimation of the η factor

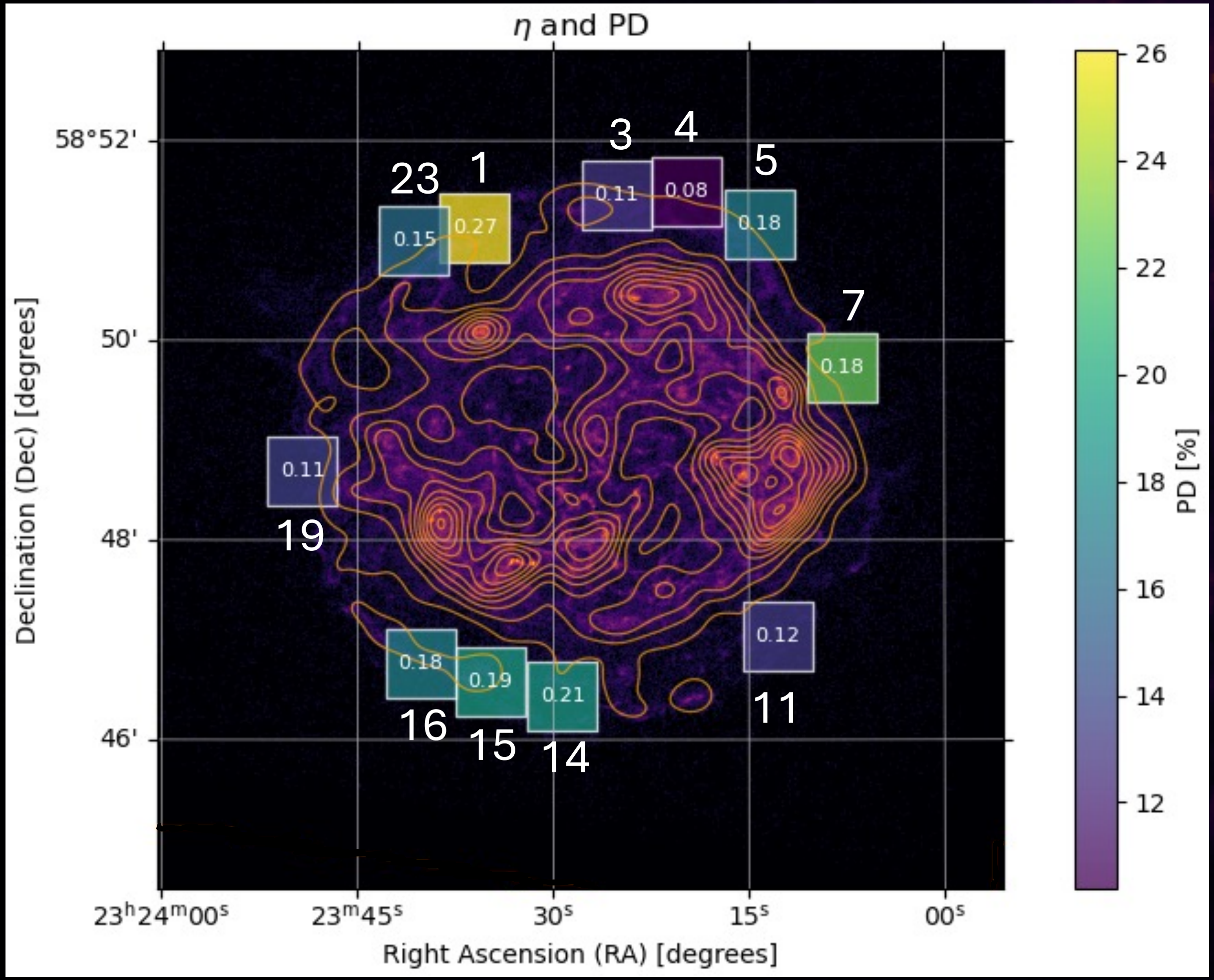

Using Bandiera & Petruk (2016), we derive the **degree of magnetic turbulence**

$$\eta = \left(\frac{B}{\delta B}\right)^2$$

from PD under isotropic fluctuations.

$$\mathbf{PD} = \frac{s+1}{s+7/3}\,\frac{5+s}{8}\,\frac{3\,B^2}{2\,\delta B^2}\,\frac{{}_1F_1\left(\frac{(3-s)}{4},3,-\frac{3\,B^2}{2\,\delta B^2}\right)}{{}_1F_1\left(-\frac{(1+s)}{4},3,-\frac{3\,B^2}{2\,\delta B^2}\right)}$$

where s is the spectral index ($s = 2\Gamma - 1$),
Γ is the photon index from Chandra data analysis.

> η < 1 → δB >> B
>
> → Fluctuating field stronger than the mean field.

Ongoig investigation

P.25

We investigate X-ray synchrotron emission in Cassiopeia A to constrain magnetic fields, diffusion lengths, and to explore their link to particle transport and X-ray polarization.

Magnetic field damping

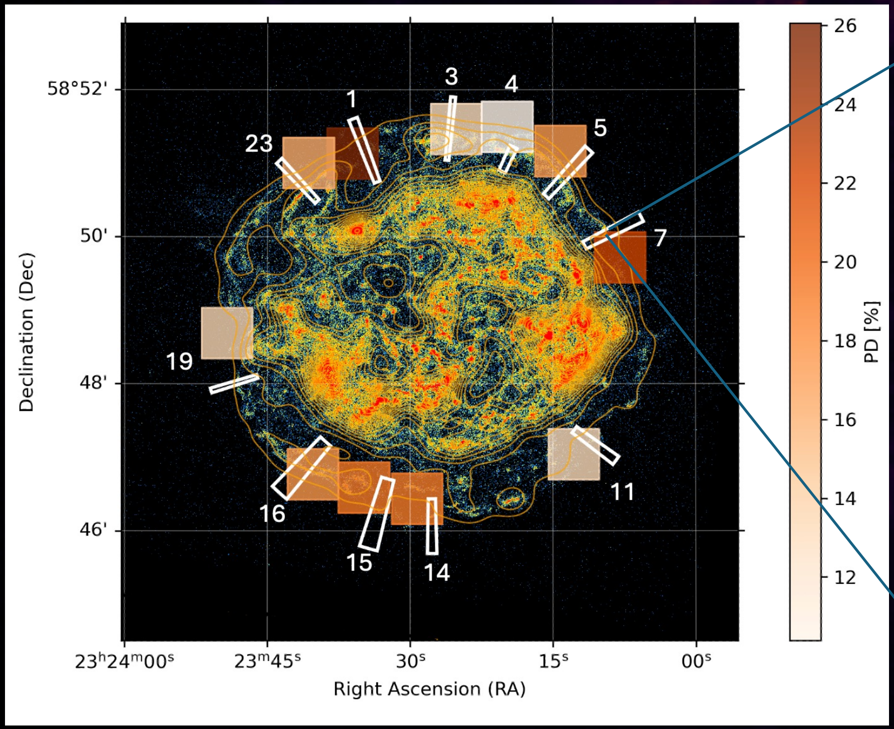

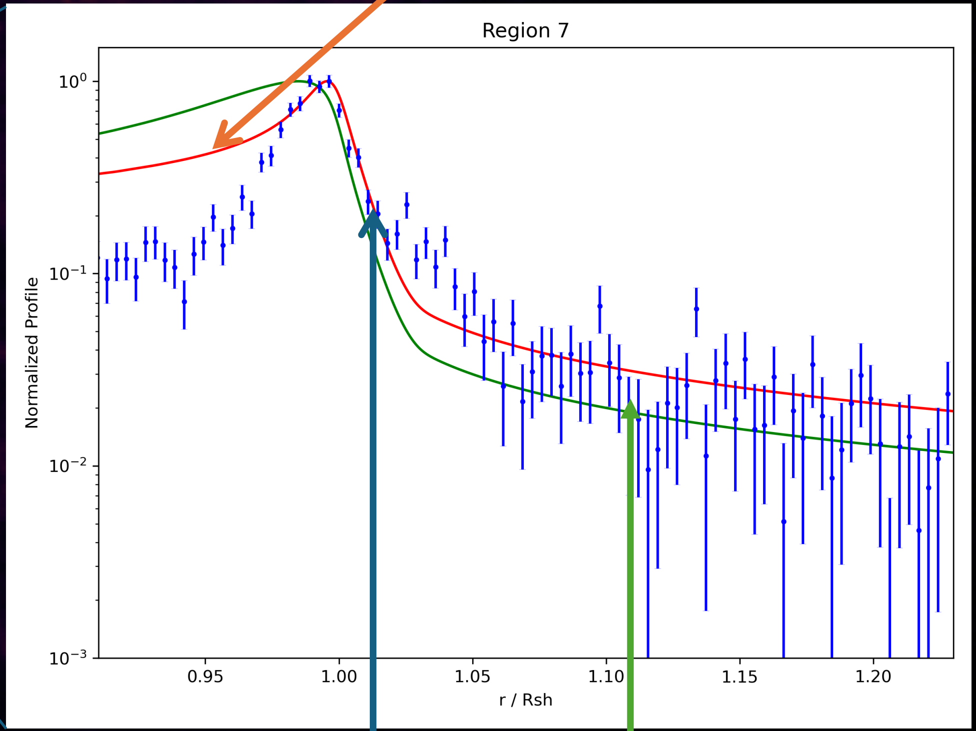

Diffusive regime

Superdiffusive regime

Ongoig investigation

P.25

We investigate X-ray synchrotron emission in Cassiopeia A to constrain magnetic fields, diffusion lengths, and to explore their link to particle transport and X-ray polarization.

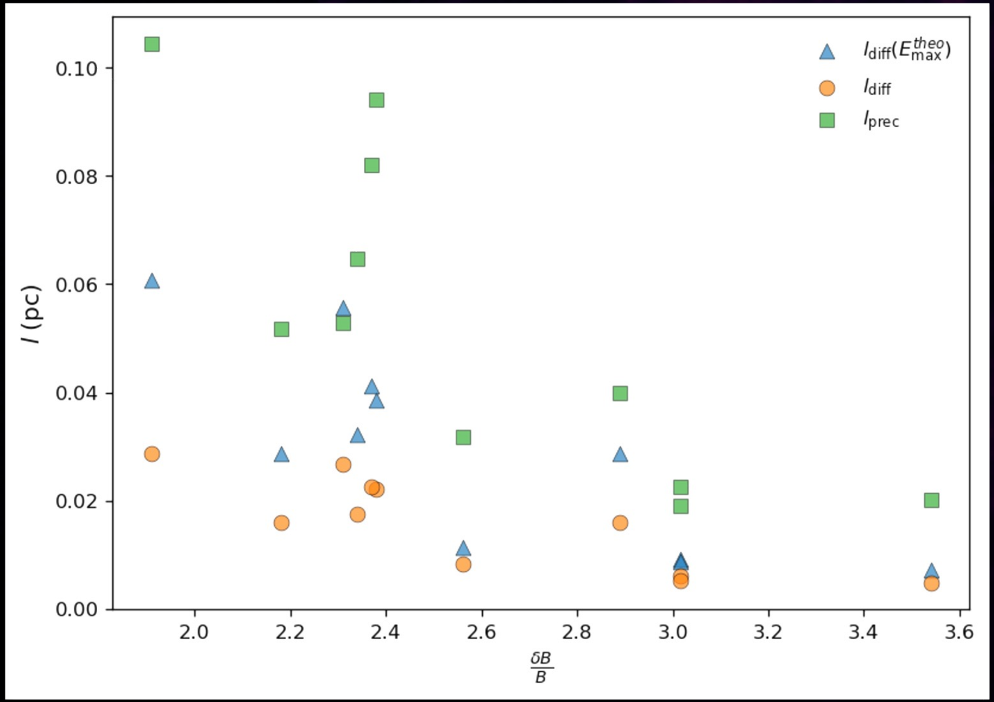

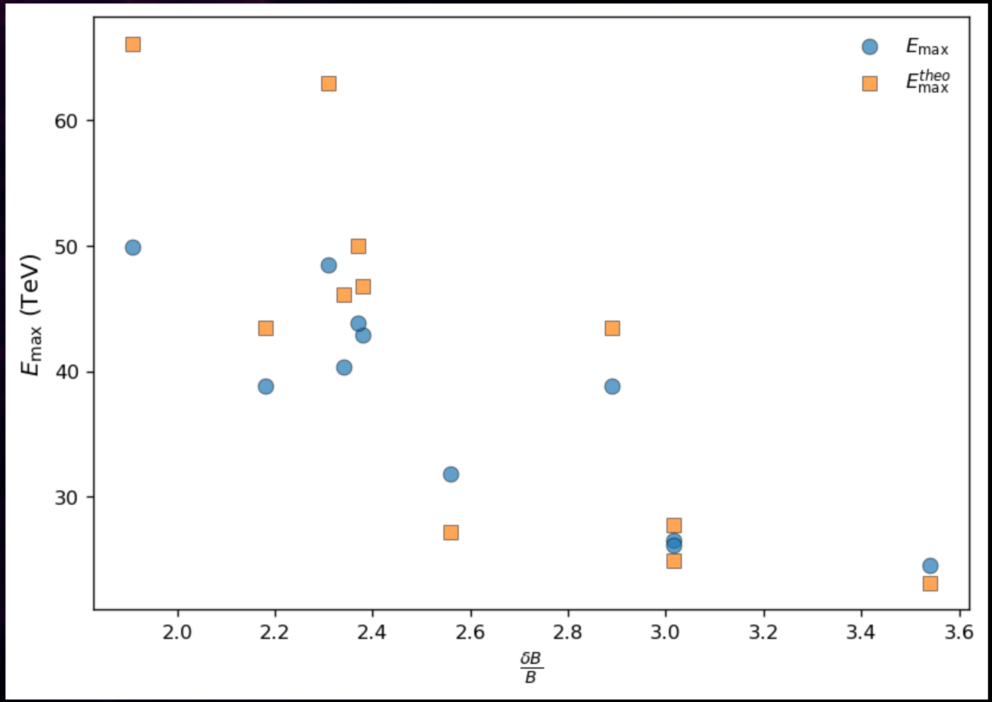

Conclusions

1. Polarization Degree (PD) and Magnetic Fields:

1. Vink et al. (2022) reported an average PD of 5%, but our analysis shows PD can reach up to **26% near the forward shock**, with PA consistently aligning with a **radial magnetic field**.
2. **West regions**, near the counter-jet, exhibit **tangential magnetic fields**, likely due to complex local dynamics.

Conclusions

1. **Polarization Degree (PD) and Magnetic Fields:**
    1. Vink et al. (2022) reported an average PD of 5%, but our analysis shows PD can reach up to **26% near the forward shock**, with PA consistently aligning with a **radial magnetic field**.
    2. **West regions**, near the counter-jet, exhibit **tangential magnetic fields**, likely due to complex local dynamics.

2. **Highest Polarization in Northeast and Southeast**:
    1. Northwest region shows lower PD due to turbulent fields from shock-CSM interactions.

Conclusions

1.Polarization Degree (PD) and Magnetic Fields:

1. Vink et al. (2022) reported an average PD of 5%, but our analysis shows PD can reach up to **26% near the forward shock**, with PA consistently aligning with a **radial magnetic field**.
2. **West regions**, near the counter-jet, exhibit **tangential magnetic fields**, likely due to complex local dynamics.

2.Highest Polarization in Northeast and Southeast:

1. Northwest region shows lower PD due to turbulent fields from shock-CSM interactions.

3.Spectropolarimetric Approach:

1. Our method detects **more regions with significant polarization** than IXPEOBSSIM.
2. PA results are consistent between both methods, showing that the **thermal component** affects PD but not PA.

Conclusions

1. Polarization Degree (PD) and Magnetic Fields:

1. Vink et al. (2022) reported an average PD of 5%, but our analysis shows PD can reach up to **26% near the forward shock**, with PA consistently aligning with a **radial magnetic field**.
2. **West regions**, near the counter-jet, exhibit **tangential magnetic fields**, likely due to complex local dynamics.

2. Highest Polarization in Northeast and Southeast:

1. Northwest region shows lower PD due to turbulent fields from shock-CSM interactions.

3. Spectropolarimetric Approach:

1. Our method detects **more regions with significant polarization** than IXPEOBSSIM.
2. PA results are consistent between both methods, showing that the **thermal component** affects PD but not PA.

4. Magnetic Turbulence (η):

1. **$\eta < 1 \rightarrow \delta B >> B$** , indicating **high turbulence** across Cas A. Results align with Ferrazzoli et al. (2023) for Tycho's SNR.

How to estimate the thermal contribution?

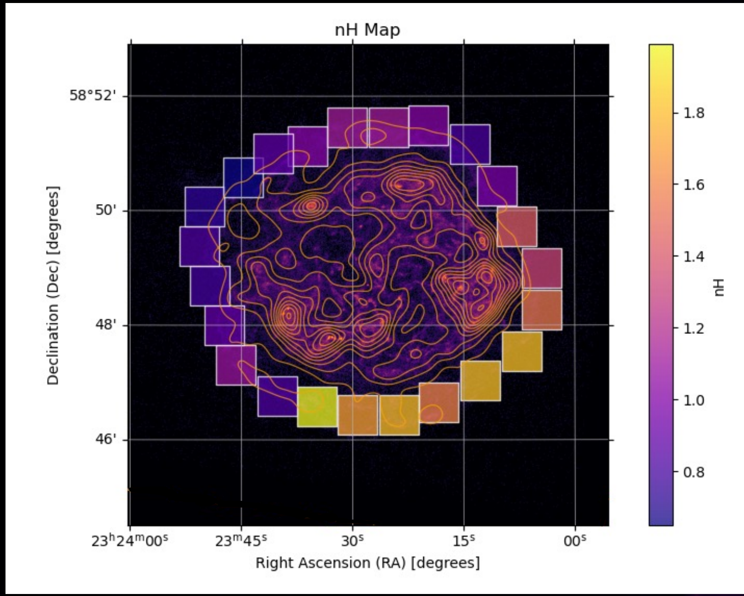

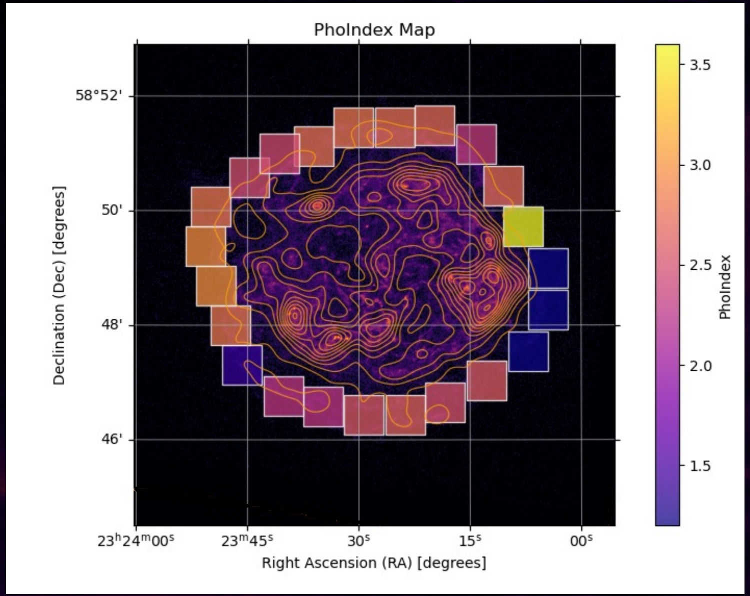

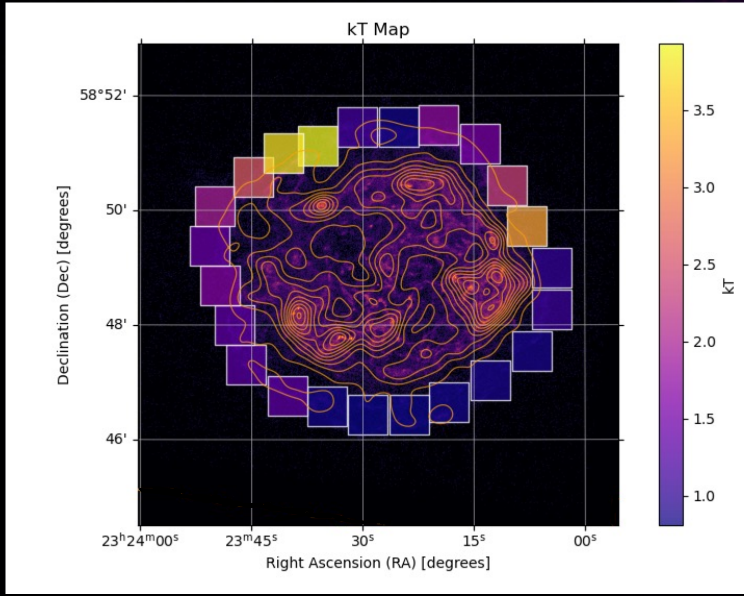

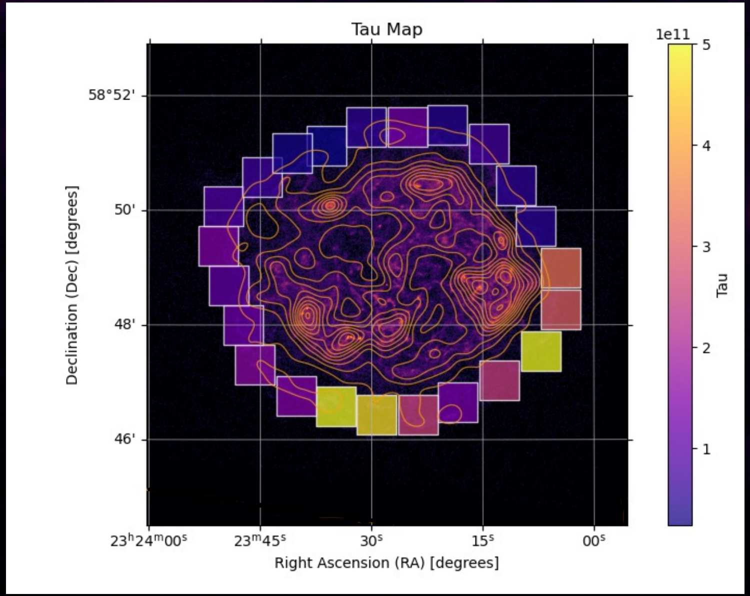

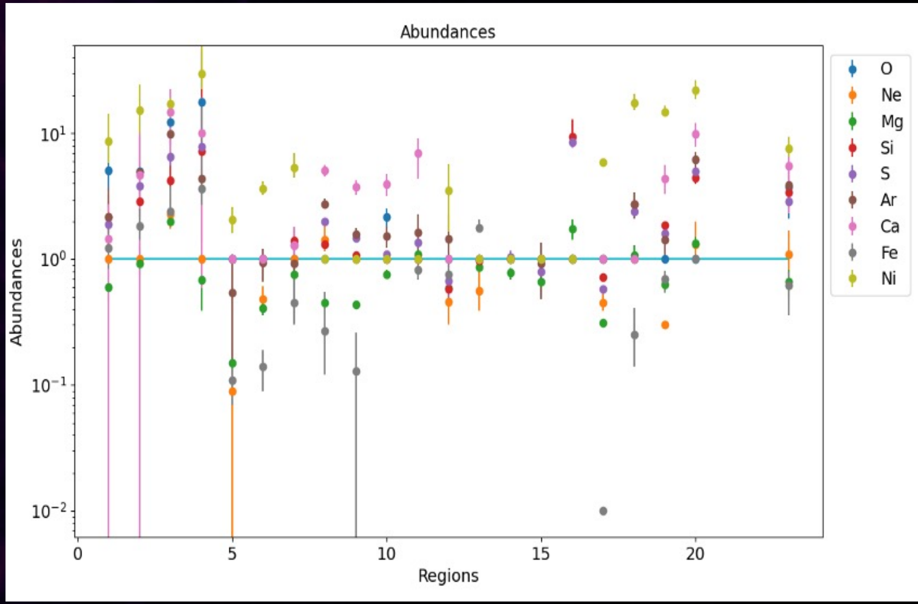

Chandra Spectral Fitting

Model Used:
TBabs*(vnei+powerlaw)

Tbabs

The *'Tbabs'* model is used to calculate the absorption of X-rays as they pass through the ISM.

The mechanisms of X-ray absorption include both photoelectric absorption and scattering.

The model calculates the cross section for X-ray absorption by the ISM as

$$\sigma_{ISM} = \sigma_{gas} + \sigma_{molecules} + \sigma_{grains}$$

The observed X-ray spectrum of a source is

$$I_{obs}(E) = e^{-\sigma_{ISM}\, nH} I_{source}(E)$$

The only parameter in this model is the hydrogen column nH $\left(\frac{10^{22} atoms}{cm^{-2}}\right)$.

Wilms et al. 2000

VNEI

VNEI is a non-equilibrium ionization collisional plasma model, that assumes a constant temperature of the gas. It provides a characterization of the spectrum but is not a physical model.

The fundamental parameters are:

- the plasma temperature kT (keV);
- the metal abundances: the elements included are H, He, C, N, O, Ne, Mg, Si, S, Ar, Ca, Fe, Ni
- the density-weighted ionization timescale, Tau , in units of s/cm^3 ;
- the redshift;
- the normalization defined as $\mathrm{n}orm = \frac{10^{-14}}{4\pi[D_A(1+z)]^2}\int n_e n_H d\,V \quad (photons/cm^2 s\,)$.

powerlaw

This component is made of a simple power-law in energy for the emission spectrum

$$A(E) = KE^{-\alpha}$$

modeling the non-thermal emission (synchrotron emission).
The main parameters of the model are:

- the photon index of the power-law (α) (dimensionless);
- the normalization factor (K) expressed in $photons/keV\,cm^2 s$ at 1 keV.